

A Novel Channel Estimation Scheme for OFDM/OQAM-IOTA System

SeungWon Kang and KyungHi Chang

An OFDM/offset QAM (OQAM)-IOTA system uses the isotropic orthogonal transform algorithm (IOTA) function, which has good localization properties in the time and frequency domains. This is employed instead of the guard interval used in a conventional OFDM/QAM system in order to be robust for multi-path channels. However, the conventional channel estimation scheme is not valid for an OFDM/OQAM-IOTA system due to the intrinsic inter-symbol interference of the IOTA function. In this paper, a condition is derived to reduce the intrinsic interference of the IOTA function. This condition is obtained with the proposed pilot structure used for perfect channel estimation. We also derive the preamble structure appropriate for practical channel estimation of the OFDM/OQAM-IOTA system. Simulation results show that the OFDM/OQAM-IOTA system with the proposed preamble structure performs better than the conventional OFDM system, and it has the additional advantage of an increased data transmission rate which corresponds to the guard interval retrieval.

Keywords: OFDM/OQAM, IOTA, channel estimation, preamble.

I. Introduction

Conventional OFDM/QAM systems are robust for multi-path channels due to the cyclically prefixed guard interval which is inserted between consequent symbols to cancel inter-symbol interference (ISI). However, this guard interval decreases the spectral efficiency of the OFDM system as the corresponding amount. Thus, there have been approaches of wavelet-based OFDM [1]-[5], which does not require the use of the guard interval. One approach is to use the isotropic orthogonal transform algorithm (IOTA) function as a wavelet candidate which has very good localization properties in the time and frequency domains [3]-[5] with the modulation of offset QAM (OQAM). This alternate OFDM/OQAM system with the IOTA function has better spectral efficiency than the conventional OFDM/QAM system. However, when the channel estimation scheme for the conventional OFDM/QAM system is applied straightforwardly to the OFDM/OQAM-IOTA system, intrinsic inter-symbol interference due to the characteristics of the IOTA function is observed. In this paper, a new pilot and new preamble structures are proposed for the channel estimation appropriate for an OFDM/OQAM-IOTA system.

We explain the characteristics and building blocks of the OFDM/OQAM-IOTA system in section II. In section III, the intrinsic interference characteristics of the OFDM/OQAM-IOTA system are analyzed, and the pilot structure used for perfect channel estimation and the preamble structure used for practical channel estimation in the OFDM/OQAM-IOTA system are proposed. In section IV, we validate the bit error rate (BER) performance of the OFDM/OQAM-IOTA system for the cases of the perfect channel estimation using the proposed pilot structure under an ideal channel condition and practical

Manuscript received July 06, 2006; revised Jan. 13, 2007.

SeungWon Kang (email: swkang79@hanmail.net) was with the Graduate School of IT&T, Inha University, Incheon, Korea, is now with the Department of Telecommunication Network, Samsung Electronics, S. Korea.

KyungHi Chang (phone: + 82 32 860 8422, email: khchang@inha.ac.kr) is with the Graduate School of IT&T, Inha University, Incheon, S. Korea.

channel estimation using the proposed preamble structure under a low mobility multi-path fading condition.

II. OFDM/OQAM-IOTA System

Loss of spectral efficiency due to the guard interval in the conventional OFDM/QAM system can be compensated by the use of the IOTA function, which has good localization properties in the time and frequency domains. This limits the inter-symbol interference and inter-channel interference, respectively [3]-[7]. However, the feature of the IOTA function which guarantees orthogonality only on real values causes the IOTA function to be used with OFDM/OQAM. Real and imaginary values are separated by the duration of half a symbol in order to preserve the orthogonality between them, as shown in Fig. 1 [5].

In Fig. 1, τ_0 and T_u denote the effective symbol durations of the OFDM/OQAM and the conventional OFDM/QAM,

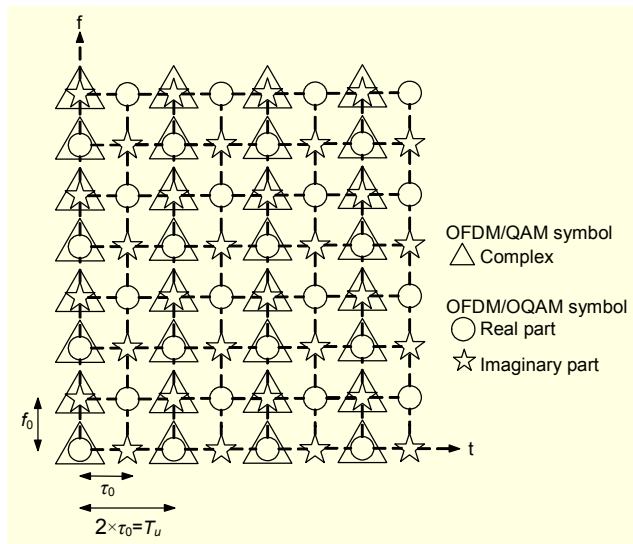


Fig. 1. Signal structure of the OFDM/OQAM system in time and frequency domains [5].

respectively. While conventional OFDM/QAM has a complex value every $2\tau_0 + \Delta$ (Δ is the guard interval), OFDM/OQAM has a real value every τ_0 , and the sub-carrier spacing of both systems is f_0 .

Figure 2 shows a functional block diagram of the OFDM/OQAM-IOTA system, where the IOTA functions are located after inverse fast Fourier transform (IFFT) in the transmitter and before FFT in the receiver of the OFDM/OQAM-IOTA system. Functional blocks specific to the OFDM/OQAM-IOTA system are represented by the dotted blocks. In Fig. 2, $s(t)$ and $s_{IOTA}(t)$ denote the transmitted signal of the OFDM/OQAM-IOTA system before and after the IOTA function, respectively; $r_{IOTA}(t)$ denotes the received signal of the OFDM/OQAM-IOTA system before the IOTA function in the receiver; and $r(t)$ and r_{FFT} denote the received signal of the OFDM/OQAM-IOTA system before and after FFT, respectively.

$$s(t) = \sum_n \sum_{m=0}^{M-1} a_{m,n} i^{m+n} e^{(2i\pi m \Delta f t)} \quad (1)$$

$$s_{IOTA}(t) = \sum_n \sum_{m=0}^{M-1} a_{m,n} i^{m+n} e^{(2i\pi m \Delta f t)} \mathfrak{I}_{m,n}(t - n\tau_0) \quad (2)$$

$$r_{IOTA}(t) = \sum_n \sum_{m=0}^{M-1} H_{m,n} s_{IOTA}(t) + n(t) \quad (3)$$

$$r(t) = \mathfrak{I}_{m,n}(t) * r_{IOTA}(t) \quad (4)$$

Equation (1) denotes the transmitted signal in which $a_{m,n}$ represents the real-valued information in the OFDM/OQAM-IOTA system sent on the m -th sub-carrier at the n -th symbol, i^{m+n} dephases $a_{m,n}$, M is the number of sub-carriers, and Δf is the sub-carrier spacing. Equation (2) denotes the transmitted signal processed with the IOTA function $\mathfrak{I}_{m,n}(t)$, where IOTA function $\mathfrak{I}_{m,n}(t)$ is used for the signal sent on the m -th

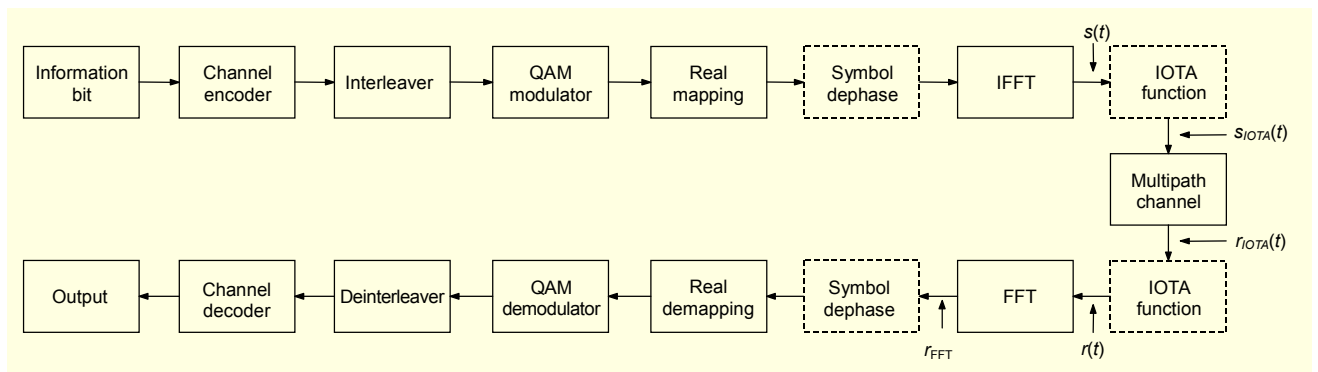


Fig. 2. Functional block diagram of the OFDM/OQAM-IOTA system.

sub-carrier at the n -th symbol, instead of inserting the guard interval. Equation (3) denotes the received signal through the multi-path fading channel, where $H_{m,n}$ and $n(t)$ are the channel gain and AWGN, respectively. Equation (4) denotes the received signal processed with the same IOTA function $\mathfrak{S}_{m,n}(t)$ at the receiver, where $*$ represents a convolution operation.

III. Proposed Preamble Structure for Practical Channel Estimation in OFDM/OQAM-IOTA System

When the channel estimation scheme for the conventional OFDM/QAM system is applied straightforwardly to the OFDM/OQAM-IOTA system, intrinsic interference due to the IOTA function is observed [4]. To observe the effects of the intrinsic interference in the OFDM/OQAM-IOTA system, we assume that there is no distortion due to the channel; this is termed the ideal channel. The received signal via the ideal channel should be equal to the transmitted signal for the conventional transmission system.

$$\begin{aligned} r_{FFT} &= \int r_{IOTA}(t) \mathfrak{S}_{m_0, n_0}(t) i^{m+n} e^{-(2i\pi m \Delta f t)} dt \\ &= \int s_{IOTA}(t) \mathfrak{S}_{m_0, n_0}(t) i^{m+n} e^{-(2i\pi m \Delta f t)} dt \\ &= a_{m_0, n_0} + \underbrace{\sum_{(m,n) \neq (m_0, n_0)} a_{m,n} \int \mathfrak{S}_{m,n} \mathfrak{S}_{m_0, n_0} dt}_{I_{m_0, n_0}} \end{aligned} \quad (5)$$

Equation (5) denotes the signal demodulated by FFT at the receiver under the ideal channel condition. In (5), m_0 and n_0 represent the sub-carrier and symbol indices that are affected by the interference of the IOTA function, respectively. Thus, $\mathfrak{S}_{m_0, n_0}(t)$ represents the IOTA function used to recover the signal sent on the m_0 -th sub-carrier at the n_0 -th symbol, a_{m_0, n_0} denotes the signal sent on the m_0 -th sub-carrier at the n_0 -th symbol, and I_{m_0, n_0} denotes total intrinsic interference on a_{m_0, n_0} . In the conventional transmission system, the values of I_{m_0, n_0} become zero under this ideal channel. However, in the OFDM/OQAM-IOTA system, intrinsic interference values I_{m_0, n_0} , which come from the neighboring sub-carriers, become non-negligible, and the values are composed of purely imaginary values.

If the perfect channel estimation for the OFDM/OQAM-IOTA system is performed with the conventional pilot structure shown in Fig. 3 for both odd and even symbols under the ideal channel condition [4], we obtain the estimated channel gain as shown in Fig. 4. In Fig. 3, all of the pilots have a value of $+\sqrt{e}$ or $-\sqrt{e}$, and e denotes the energy of each pilot tone. In

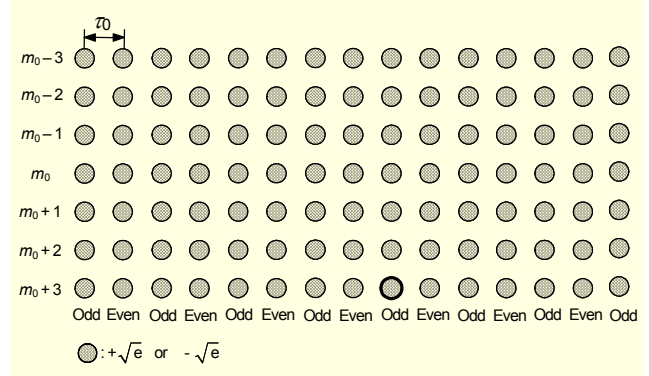


Fig. 3. Conventional pilot structure used for the perfect channel estimation. All of the pilots are $+\sqrt{e}$ or $-\sqrt{e}$.

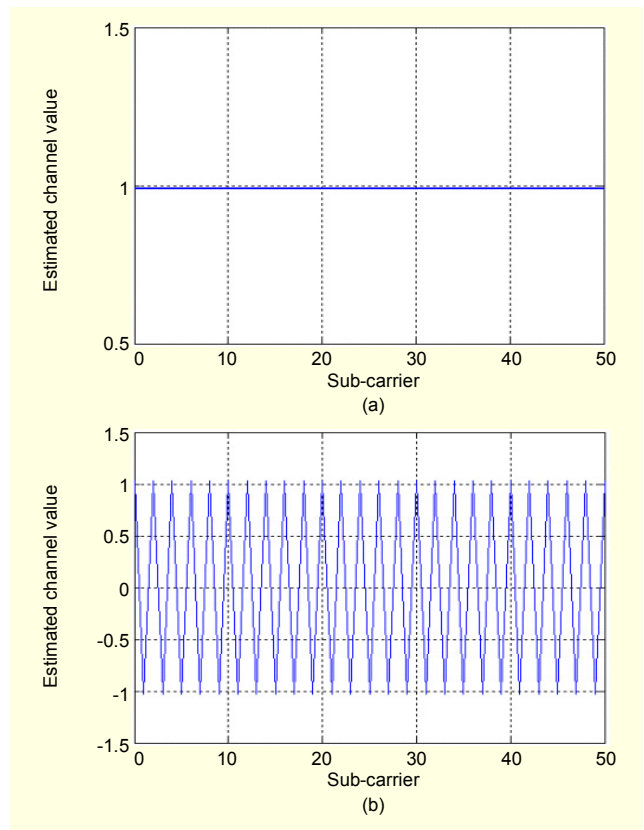


Fig. 4. Estimated channel gain with conventional pilot structure for perfect channel estimation under ideal channel condition: (a) estimated channel gain in real part and (b) in imaginary part.

this paper, we define the perfect channel estimation as a channel estimation using the pilot existing on every grid point of a sub-carrier and a symbol as in Fig. 3. Under the ideal channel condition, channel gain becomes $1+j_0$. However, the imaginary part of the channel gain shown in Fig. 4(b) oscillates between -1 and 1 according to the sub-carriers. That is, intrinsic interference is observed only in the imaginary part as shown in Fig. 4(b). Therefore, the occurrence of intrinsic interference is

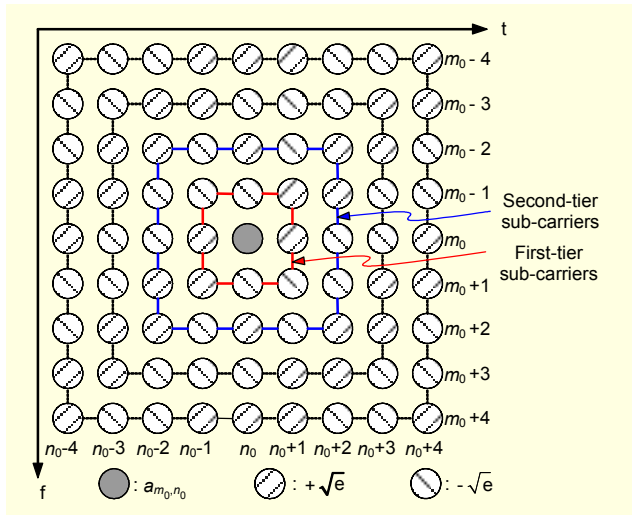


Fig. 5. Prototype preamble structure which makes interference coming from the neighboring sub-carriers zero.

due to the IOTA function, which has orthogonality on only the real values; thus, the interference appears on the imaginary part of the information. Equation (6) represents the total interference, where C_{m_0, n_0}^1 and D_{m_0, n_0} represent the interference which comes from the first-tier sub-carriers and the sub-carriers at the residual tiers, respectively. Here, Ω_{m_0, n_0}^1 represents the indices of the first-tier sub-carriers as shown in Fig. 5. To perform the channel estimation on a_{m_0, n_0} correctly, which represent the real-valued information of the OFDM/OQAM-IOTA system sent on the m_0 -th sub-carrier at the n_0 -th symbol, a pilot structure that makes I_{m_0, n_0} zero is required. Figure 5 shows one of the prototype preamble structures which make interference coming from the neighbor sub-carriers zero. However, the more tiers that are considered as sources of interference in a preamble, the lower spectral efficiency is with a longer preamble. Therefore, it is important to decide the number of tiers to be considered as major sources of interference.

$$I_{m_0, n_0} = C_{m_0, n_0}^1 + D_{m_0, n_0}, \quad (6)$$

where

$$C_{m_0, n_0}^1 = \sum_{(m, n) \in \Omega_{m_0, n_0}^1} a_{m, n} \int \Im_{m, n} \Im_{m_0, n_0}^* dt.$$

To create the pilot structure canceling interference from neighboring sub-carriers, we derive the required condition to make I_{m_0, n_0} of (6) equal to zero on a_{m_0, n_0} by utilizing the prototype preamble structure shown in Fig. 5. Then, the condition to make interference coming from all neighboring sub-carriers equal to zero in the OFDM/OQAM-IOTA system is derived as.

$$\begin{aligned} & \sum_{j=0}^{m_0-1} \sum_{i=1}^{n_0-1} \sum_{k=1}^2 \left\{ a_{m_0+(-1)^k j, n_0+i} + (-1)^{j+1} a_{m_0+(-1)^k j, n_0-i} \right\} \\ & + \sum_{j=0}^{m_0-1} (a_{m_0+j, n_0} - a_{m_0-j, n_0}) \\ & = \sum_{j=0}^{m_0-1} \sum_{i=1}^{n_0-1} \left\{ a_{m_0+j, n_0+i} + (-1)^{j+1} a_{m_0+j, n_0-i} \right\} \\ & + \sum_{j=1}^{m_0-1} \sum_{i=1}^{n_0-1} \left\{ a_{m_0-j, n_0+i} + (-1)^{j+1} a_{m_0-j, n_0-i} \right\} \\ & + \sum_{j=0}^{m_0-1} (a_{m_0+j, n_0} - a_{m_0-j, n_0}) \\ & = 0. \end{aligned} \quad (7)$$

However, the pilot structure satisfying (7) can be constructed only in the case of perfect channel estimation due to its complex relationship. For this reason, we suggest that channel estimation in the OFDM/OQAM-IOTA system is better achieved using a preamble instead of using pilots. The simulation results for the OFDM/OQAM-IOTA system demonstrate that this approach is more suitable for application in low mobility conditions.

Due to the good localization properties of the IOTA function, it is assumed that major interference comes from the first-tier sub-carriers around the (m_0, n_0) sub-carrier [4]. To derive the optimized preamble structure, the creation of a pilot structure assuming the perfect channel estimation is initially attempted. That is, a pilot structure to make C_{m_0, n_0}^1 zero is considered. Figure 6 shows the proposed even/odd center pilot structure

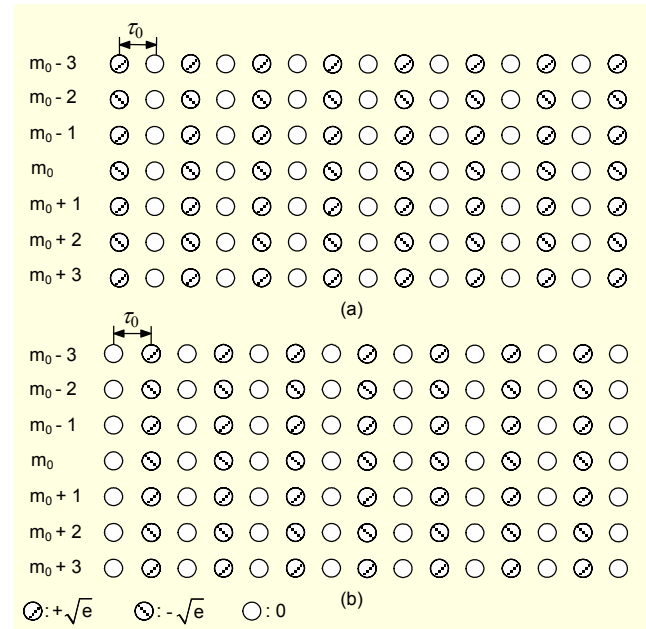


Fig. 6. Proposed pilot structure used for perfect channel estimation to cancel first-tier interference: (a) odd-center pilot structure and (b) even-center pilot structure.

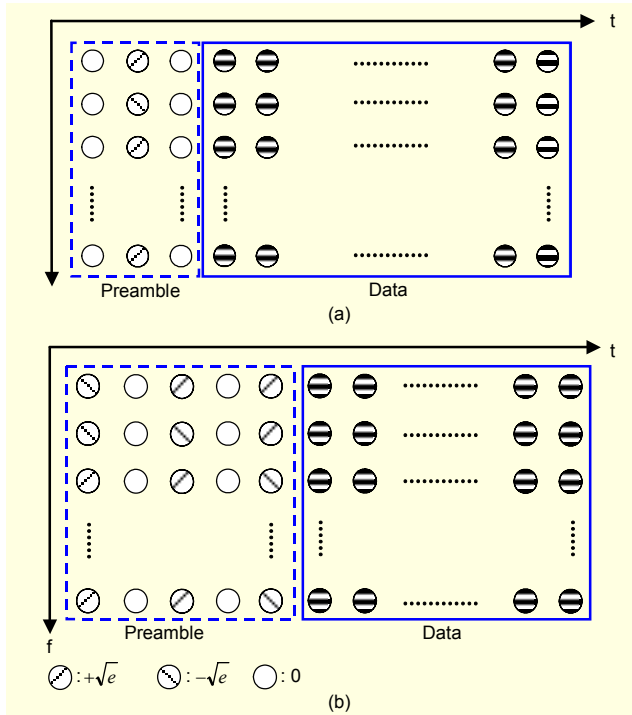


Fig. 7. Proposed preamble structure used for practical channel estimation: (a) considering first-tier sub-carriers only as major sources of interference (type 1) and (b) considering sub-carriers up to the second-tier (type 2).

satisfying (7) and Fig. 5. Each odd-center and even-center pilot serves for the channel estimation of an odd and even symbol, respectively.

Using the pilot structure shown in Fig. 6, the estimated channel gain on the real part is identical to that in Fig. 4(a), and the estimated channel gain on the imaginary part becomes negligible under the ideal channel condition, as expected. However, channel estimation using pilots in an OFDM/OQAM-IOTA system should utilize at least first-tier sub-carriers around a specific pilot, and that leads to an impractical solution due to the high density of pilots.

From the discussion above, we derive the preamble structures which are suitable for the practical channel estimation shown in Fig. 7. Figure 7(a) considers only the first-tier sub-carriers, but Fig. 7(b) considers sub-carriers up to the second tier as major sources of interference.

Where the frame lengths were set to be identical, including the preamble, Fig. 7(a) shows better spectral efficiency. The channel gain estimated using the preamble symbol in the middle is applied to the subsequent data sub-carriers in a frame to compensate the distortion due to the channel.

IV. Performance Validation

In this section, we validate the BER performance of the

Table 1. Fundamental simulation parameters.

Parameters	Value
Carrier frequency	2.4 GHz
FFT size	512
Sampling frequency	76.8 MHz
(Effective) Symbol duration	6.67 μ s
Guard interval (for conventional OFDM)	128 samples (1.67 μ s)
Number of data symbols in a frame	12 symbols
Frame duration :	- 108.42 μ s
- Conventional OFDM	- Type 1: 100.05 μ s
- OFDM/OQAM-IOTA	- Type 2 : 113.39 μ s
Modulation	QAM / OQAM
Prototype function	IOTA function
Channel coding	Uncoded
Channel estimation	Perfect / Practical
Fading channel	ITU-R Veh-A (Max. delay spread: 1.09 μ s)
Mobility	10 km/h

OFDM/OQAM-IOTA system for cases of perfect channel estimation using the proposed pilot structure under the ideal channel condition, as well as for practical channel estimation using the proposed preamble structure under a low mobility multi-path fading channel. The BER performance of the OFDM/OQAM-IOTA system, considering only the first-tier sub-carriers and the sub-carriers up to the second-tier as major sources of interference, is also compared.

Table 1 shows the fundamental simulation parameters for performance validation, in which types 1 and 2 represent a frame structure shown in Fig. 7. A frame consists of a preamble and 12 data symbols. Compared to the preamble length of one symbol in the conventional OFDM/QAM system, the lengths of preambles in the OFDM/OQAM-IOTA system considered in this paper are 3 symbols and 5 symbols corresponding to the frame structures of type 1 and type 2, respectively. Two symbol duration in the OFDM/OQAM-IOTA system corresponds to 1-symbol duration in the OFDM/QAM system.

1. Perfect Channel Estimation

Figure 8 shows the BER performance of the perfect channel estimation in the OFDM/OQAM-IOTA system with the proposed pilot structure shown in Fig. 6 under flat Rayleigh fading channel. The BER performance of the perfect channel estimation is nearly identical to the theoretical value of QPSK as expected, because there is no loss of power due to the guard interval.

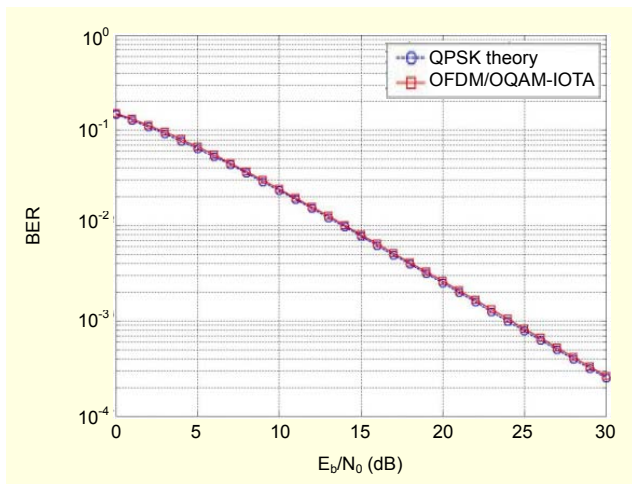


Fig. 8. BER performance of perfect channel estimation in OFDM/OQAM-IOTA system under the flat Rayleigh fading channel.

2. Practical Channel Estimation

Figure 9 shows the BER performance of the OFDM/OQAM-IOTA system under flat and 4-path Rayleigh fading channels, considering only the first-tier sub-carriers as major sources of interference. At the target BER of 10^{-3} , simulation results show that the OFDM/OQAM-IOTA system with the proposed preamble structure has approximately 1.5 dB and 1.4 dB of E_b/N_0 gain in flat and 4-path Rayleigh fading channels, respectively. This is primarily due to the greater robustness of the OFDM/OQAM-IOTA system to ICI. For reference, signal power loss due to the guard interval in this example of the conventional OFDM/QAM system is 0.97 dB. Moreover, the OFDM/OQAM-IOTA system, considering only the first-tier sub-carriers as major sources of interference, preserves a nearly 35% increase in the data transmission rate per frame compared to the conventional OFDM/QAM system. Moreover, as the number of data symbols per frame increases, the improvement in the data transmission rate compared to the conventional OFDM/QAM system also increases.

The BER performance of the OFDM/OQAM-IOTA system considering only the first-tier sub-carriers and sub-carriers up to the second-tier as major sources of interference under flat and 4-path Rayleigh fading channels is shown in Fig. 10. From Fig. 10, we can conclude that considering only the first-tier sub-carriers as major sources of interference is sufficient due to the good localization properties of the IOTA function.

V. Conclusion

In this paper, we presented a prototype preamble structure, and derived a condition to make the intrinsic interference of the

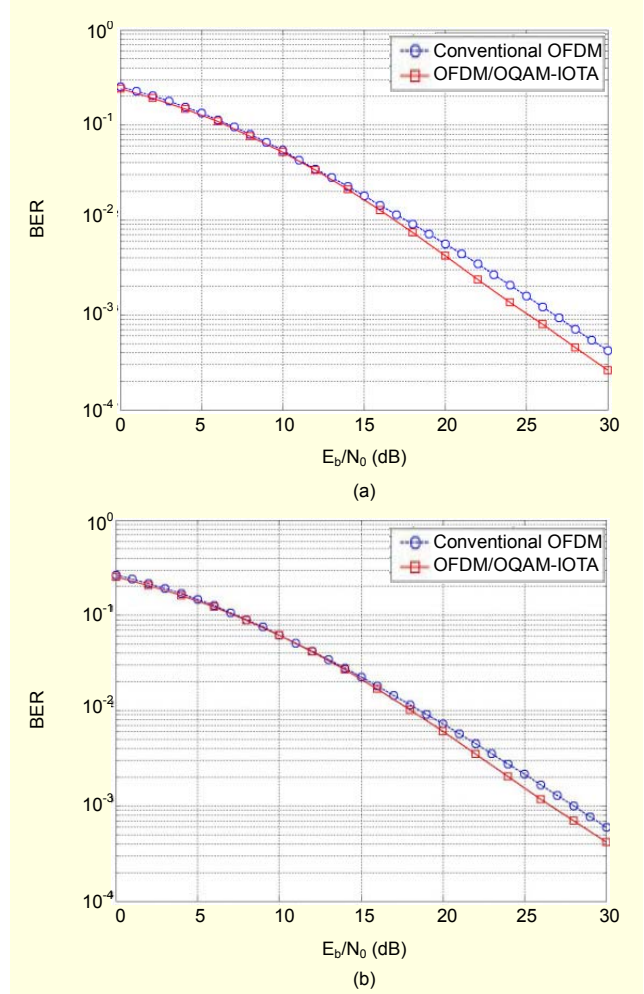


Fig. 9. BER performance of conventional OFDM/QAM system vs. OFDM/OQAM-IOTA system considering only first-tier sub-carriers as major sources of interference: (a) flat Rayleigh fading channel and (b) 4-path Rayleigh fading channel.

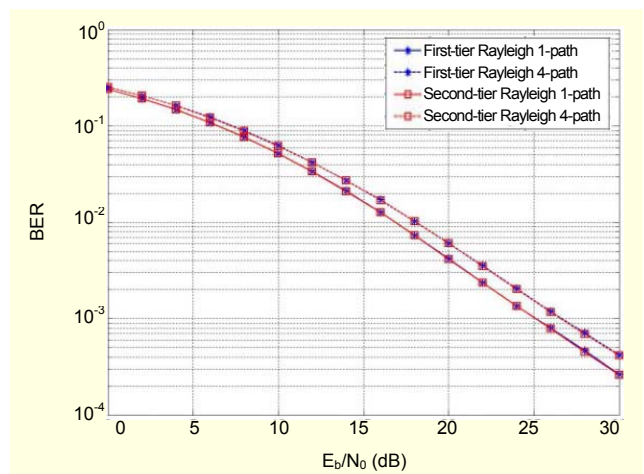


Fig. 10. BER performance of OFDM/OQAM-IOTA system considering first-tier sub-carriers only and sub-carriers up to the second-tier as major sources of interference.

IOTA function zero. Based on the proposed pilot structure used for the perfect channel estimation, we additionally derived a preamble structure appropriate for practical channel estimation for the OFDM/OQAM-IOTA system. Simulation results show that the OFDM/OQAM-IOTA system with the proposed preamble structure performs better than the conventional OFDM system, with the additional advantage of an increased data transmission rate which corresponds to the guard interval retrieval.

References

- [1] H. Zhang, D. Yuan, M. Jiang, and D. Wu, "Performance Comparison of WOFDM with Different Coding Schemes," *Proc. RAWCON*, Aug. 2003, pp. 59-62.
- [2] T. Kurt, M. Siala, and A. Yongacoglu, "Multi-Carrier Signal Shaping Employing Hermite Functions," *Proc. EUSIPCO*, Sep. 2005.
- [3] C. Roche and P. Siohan, "A Family of Extended Gaussian Functions with a Nearly Optimal Localization Property," *Proc. First Int. Workshop Multi-Carrier Spread-Spectrum*, Oberpfaffenhofen, Germany, Apr. 1997, pp. 179-186.
- [4] D. Lacroix and J.P. Javardin, "A New Channel Estimation Method for OFDM/OQAM," *Proc. Int. OFDM Workshop*, Sep. 2002.
- [5] J.P. Javardin and D. Lacroix, "Technical Description of the OFDM/IOTA Modulation," *3GPP TSG-RAN-1 Meeting #31*, Tokyo, Japan, Feb. 2003.
- [6] P. Siohan and C. Roche, "Cosine-Modulated Filterbanks Based on Extended Gaussian Functions," *IEEE Trans. Signal Processing*, vol. 48, Nov. 2000, pp. 3052-3061.
- [7] P. Siohan and C. Roche, "Derivation of Extended Gaussian Functions Based on the Zak Transform," *IEEE Signal Processing Lett.*, vol. 11, Mar. 2004, pp. 401-403.



SeungWon Kang received the BS degree in electronics engineering from Inha University, Incheon, Korea, in 2005. He received the MS degree in the Graduate School of Information Technology and Telecommunications, Inha University, Incheon, Korea, in 2007. He is currently with the Telecommunication Network (TN), Samsung Electronics Co., Ltd. His research interests include 4G wireless communication systems, MIMO techniques, turbo equalizer, WiBro, and wavelet-based OFDM systems.



KyungHi Chang received the BS and MS degrees in electronics engineering from Yonsei University, Seoul, Korea, in 1985 and 1987, respectively. He received his PhD degree in electrical engineering from Texas A&M University, College Station, Texas, in 1992. From 1989 to 1990, he was with the Samsung Advanced Institute of Technology (SAIT) as a member of research staff and was involved in digital signal processing system design. From 1992 to 2003, he was with the Electronics and Telecommunications Research Institute (ETRI) as a principal member of technical staff. During this period, he led the team of WCDMA UE modem design and 4G radio transmission technology (RTT). He is currently with the Graduate School of Information Technology and Telecommunications, Inha University, where he has been an associate professor since 2003. His current research interests include RTT design for IMT-Advanced & 3GPP LTE systems, WMAN system design, cognitive radio, cross-layer design, and cooperative relaying systems. Dr. Chang has served as a senior member of IEEE since 1998. Currently he is Editor-in-Chief for the Korean Institute of Communication Sciences (KICS) Proceedings. He has also served as an editor of ITU-R TG8/1 IMT.MOD, and he is currently an International IT Standardization Expert of the Telecommunications Technology Association (TTA).